Journal of Chromatography, 353 (1986) 439–463
Elsevier Science Publishers B.V., Amsterdam — Printed in The Netherlands

CHROMSYMP. 690

SEPARATION OF PROTEINS BY GRADIENT ELUTION FROM ION-EXCHANGE COLUMNS

OPTIMIZING EXPERIMENTAL CONDITIONS

R. W. STOUT*, S. I. SIVAKOFF and R. D. RICKER
Biomedical Products Department, E. I. du Pont de Nemours & Co., Inc., Wilmington, DE 19898 (U.S.A.)
and
L. R. SNYDER
LC Resources, Inc., 26 Silverwood Court, Orinda, CA 94563 (U.S.A.)

SUMMARY

A model has been described previously for the gradient elution separation of large biomolecules by reversed-phase high-performance liquid chromatography. This model has now been adapted to the special case of ion-exchange separation with linear salt gradients and protein samples. Application to experimental data from the gradient separation of various proteins shows good agreement with the model for both retention and bandwidth data. A computer program has been written, based on the model, that allows predictions of how separation changes with experimental conditions. This program can be used to aid method development for ion-exchange gradient separations of protein samples. We have also used the program to explore strategies for the best approach to method development for these separations. Final recommendations are summarized.

INTRODUCTION

High-performance liquid chromatography (HPLC) in the ion-exchange mode is now commonly used for the separation and purification of protein samples[1–5]. Relatively high resolution is possible with this technique, and separated proteins can be recovered in good yield with little loss of bioactivity. That is, unlike the case of reversed-phase HPLC, protein samples are not normally denatured in ion-exchange chromatography.

Ion-exchange protein separations exhibit features that appear to differ in some respects from what might be expected for small-molecule ion-exchange HPLC. Thus, Kopaciewicz *et al.*[6] have shown that retention is not governed by the net charge on the protein molecule as is the case in inorganic ionic species[7], but rather by the effective charge on one part of the protein molecule. Gooding and Schmuck[8] have further shown an unusual dependence of relative retention and bandwidth on the ionic composition (kind of salt) of the mobile phase in ion-exchange separations of

0021-9673/86/$03.50

several proteins. Kato *et al.*[9] have studied retention and bandwidth as a function of gradient conditions in the separation of a crude ovalbumin sample by anion exchange, but the authors did not comment on any peculiarities in their data.

We suggested earlier[10] that gradient separations of proteins by ion-exchange HPLC can be interpreted in terms of conventional chromatographic theory[11]. Subsequently, we have developed a quantitative model[12,13] for the gradient elution separation of peptides and proteins by reversed-phase HPLC. This model allows the quantitative prediction of both retention and bandwidth as a function of experimental conditions. We have further used the model to construct a computer program that allows accurate predictions of peak capacity (or resolution) for samples of different molecular weight, and for changes in gradient time, flow-rate, column length, and other variables[14].

In this paper, we have extended this prior treatment to include HPLC separations by ion exchange with linear salt gradients. We have also carried out a number of ion-exchange separations which allow us to test the validity of our model. Finally, a computer program has been written for these ion-exchange gradient separations that enables us to predict how a separation varies with experimental conditions. This computer program can also be used directly for facilitating method development for the gradient elution ion-exchange separation of a given sample.

THEORY

Solute retention in gradient elution

Our approach to understanding and predicting retention in gradient elution systems is based on the general theory of linear-solvent-strength (LSS) systems as presented originally in 1980[11] and elaborated upon more recently[15–18]. In LSS gradient systems, the k'-value of a solute at the column inlet (k_i) varies with time t during the gradient as

$$\log k_i = \log k_0 - b(t/t_0) \tag{1}$$

Here, k_0 is the value of k_i at the start of the gradient, t_0 is the column dead-time, and b is a constant for a given solute. Reversed-phase separations carried out with linear gradients usually adhere closely to eqn. 1, and therefore, are of the LSS type. For solutes with large values of k_0 (*i.e.*, separated under "gradient" conditions), retention time t_g for LSS systems is given as

$$t_g = (t_0/b) \log (2.3\, k_0 b) + t_0 + t_D \tag{2}$$

In the case of reversed-phase separations,

$$b = V_m \Delta\varphi S/t_G F \tag{3}$$

where V_m is column dead-volume ($V_m = t_0 F$), $\Delta\varphi$ is the total change in volume fraction φ of the organic solvent during the gradient, S is equal to $-\mathrm{d}(\log k')/\mathrm{d}t$ (constant for a given solute), t_G is the gradient time, F is the flow-rate, and t_D is the system dwell time[15].

Given two gradient runs (with t_G values of t_G1 and t_G2), eqns. 2 and 3 allow

calculation of values of k_0 and b, and from b a value of the solute parameter S can be obtained[12,17]. This allows the prediction of isocratic retention on the basis of gradient runs, as well as the extraction of isocratic parameters (k_0, S) which allow prediction of gradient retention t_g as a function of change in experimental conditions (t_G, F, V_m, etc.).

In isocratic ion-exchange chromatography (small sample sizes, assume equilibrium conditions) retention is given as a function of the concentration c of salt in the mobile phase

$$\text{(isocratic)} \qquad \log k' = \log K - m \log c \tag{4}$$

where K is the ion-exchange distribution constant and c is the concentration of salt in the mobile phase. The use of linear gradients then results in values of k_i varying with time in non-linear fashion[17], so that such separations are not of the LSS type. The LSS theory can nevertheless be adapted to deal with this situation[17,18]. It is assumed that the gradient is approximately LSS over the time during which the solute band is migrating through the column, so that eqn. 2 is obeyed over this interval. This allows solution for values of k_0 and b from each gradient run. Next, the effective (or average) k'-value of the solute during elution is determined

$$\bar{k} = 1/1.15\, b \tag{5}$$

The quantity $\bar{k}$ corresponds to the k' value of the band when it has migrated halfway along the column. The concentration c at the column midpoint when the band has reached that position is (ref. 18, or related derivation of ref. 12)

$$\bar{c} = c_0 + [t_g - t_0 - t_D - 0.30\,(t_0/b)]\,\Delta c/t_G \tag{6}$$

Here, c_0 and c_f refer to initial and final salt concentrations during the gradient, and $\Delta c = (c_f - c_0)$.

Values of $\bar{k}$ and $\bar{c}$ can thus be obtained for each gradient run, and substitution of this pair of values into eqn. 4 allows values of K and m to be obtained. Comparison of values of $\bar{c}$ *vs.* $\bar{k}$ (gradient) with corresponding isocratic data (c *vs.* k') should show close agreement (same values of K and m for each data set) if our model is correct. We have previously analyzed[17] the data of Kato *et al.*[9] in this way, and have observed that values of $\bar{k}$ and $\bar{c}$ correlate well with a single value of K and m for the column used by them; *i.e.*, demonstrating that the present approach is at least self-consistent.

Appendix I describes in detail the use of gradient retention data to extract values of $\bar{c}$, $\bar{k}$, K and m.

Solute bandwidth in gradient elution

We have previously presented a general approach to correlating and predicting bandwidth values in ion-exchange gradient elution (linear gradients, non-LSS separation)[18]. That treatment begins with the dependence of bandwidth σ_t (1 S.D. of Gaussian curve, sec) on experimental conditions in LSS gradient elution

$$\sigma_t = J\,(t_0 N^{-1/2})\, G\,[1 + (1/2.3\, b)] \tag{7}$$

Here J is an empirical parameter that recognizes "anomalous band broadening" with

TABLE I

VARIATION OF RELATIVE GRADIENT STEEPNESS (r) AND $1/\bar{k}$ AT DIFFERENT TIMES WITHIN THE GRADIENT

t/t_G*	r**-Values at the (c_f/c_0) ratios indicated			
	3	*10*	*30*	*100*
0.00	1.82	3.9	8.5	21.5
0.05	1.66	2.7	3.5	3.6
0.10	1.52	2.1	2.2	2.0
0.15	1.40	1.67	1.6	1.34
0.20	1.30	1.40	1.26	1.03
0.30	1.14	1.06	0.88	0.70
0.40	1.01	0.85	0.68	0.53
0.60	0.83	0.61	0.46	0.36
0.80	0.70	0.39	0.35	0.27
1.00	0.61	0.39	0.28	0.22

* $(t/t_G) = (c - c_0)/\Delta C$, corrected for t_0 and t_D; *i.e.*, $t = t_g - t_0 - t_D$, for approximate estimates of b_0 for a given band in the gradient.

** r is proportional to $(1/\bar{k})$.

very steep gradients*, N is the column plate number, and G is a gradient compression factor. A similar expression has been used in our previous model for reversed-phase separation[12,13]. Eqn. 7 can be used directly in ion-exchange gradient elution, if the value of b is determined from two gradient runs as described in the preceding section. Alternatively, we will be interested in estimating b for a single gradient run[18].

First, consider an average value of b for the entire gradient run. If the gradient were of the LSS type from beginning to end (*i.e.*, concave salt gradient), b would be given by (*cf.* eqn. 3 for reversed-phase HPLC)

$$b = V_m \log (c_f/c_0)/t_G F \tag{8}$$

In the case of a linear salt gradient, b will not be constant over the entire gradient, but will vary from beginning to end. We can define an "actual" value of b (b_0) which is related to the average value of b (eqn. 8) as

$$b_0 = rb \tag{9}$$

where

$$r = \Delta c/2.3\ c \log (c_f/c_0) \tag{10}$$

The variation of r with position within the gradient (t/t_G) is given in Table I. Since $\bar{k}$ is approximately equal to $1/b$ (eqn. 5), it is seen that for a given value of b (eqn. 8), $\bar{k}$ increases with (t/t_G). We will comment on this in the following section.

* J has been found[13] to be a function only of gradient steepness b. In the present study values of b varied from 0.2 (shallow gradient) to 1.4 (fairly steep), with J varying from 1.4 to 1.8. Thus experimental values of σ_t were predicted (and found) to be 1.4–1.8-fold greater than calculated by eqn. 7 with $J = 1$ ($J = 1$ means no anomalous band broadening).

We can obtain an exact value of σ_t, based on an exact value of b_0, as previously described[18] and summarized in Appendix II. This approach was followed here in predictions of σ_t for comparison with actual experimental values. However, in most cases involving proteins as samples, we can approximate r from Table I, using $(t/t_G) = (t_g - t_0 - t_D)/t_G$

Appendix III describes in detail the calculation of values of σ_t based on experimental data and column parameters* (best fit values of b', A and ρ, for the DuPont columns used in the present study).

EXPERIMENTAL

Chemicals and reagents

Isocratic and gradient separations of various protein samples were carried out with mobile phases of 20 m*M* Bis-Tris (Calbiochem-Behring, La Jolla, CA, U.S.A.) containing various concentrations of sodium acetate and adjusted to pH 6.4 with sodium hydroxide or hydrochloric acid (J. T. Baker, Phillipsburg, NJ, U.S.A.). Lysozyme was purchased from Calbiochem-Behring, and ovalbumin and ribonuclease A were from Sigma (St. Louis, MO, U.S.A.). Lysozyme and ribonuclease A samples appeared not to contain major impurities that overlapped the major band in the present ion-exchange separations. Ovalbumin was a less pure sample, as can be seen from the separations of Fig. 7. Water for all applications was deionized in a Continental Water Systems unit (North Wales, PA, U.S.A.). Samples were injected as 25-μl volumes, with concentrations of about 1 mg/ml (25-μg sample injected per analysis).

Equipment

Chromatography was carried out on a Fast Protein Liquid Chromatography system (Pharmacia, Piscataway, NJ, U.S.A.), including a LCC-500 controller, two P-500 pumps, a mixer, a motor-valve MV-7 injector, a UV-1 single path monitor with a HR-10 flow cell and 280-nm filter, and a REC-482 recorder.

Data system

Analog data were digitized and archived using a Nelson Analytical 760 Series Interface (Cupertino, CA, U.S.A.), and processed with a modified version of Nelson Analytical Chromatography Software, and a HP Series 220 Microcomputer (Hewlett-Packard, Fort Collins, CO, U.S.A.). Plate number values were variously calculated by the data system (peak height/area algorithm) or directly from the chromatograms, using measured bandwidths at peak half-height ($w_{1/2}$); plate number $N = 5.56 \times (\text{retention time}/w_{1/2})^2$. Values for the same band were similar ($\pm 10\%$) by either procedure. Peak symmetry was usually good (asymmetry factors less than 1.5).

---

* The column parameters b', A, and ρ have been described previously[12,13]. The surface-diffusion parameter b' reflects the ability of sample molecules to diffuse while present in the stationary phase. The Knox parameter A is a measure of how well the column has been packed; a value of $A = 0.8$ (a "good" column) was assumed in the present study, as in ref. 13. The restricted-diffusion parameter ρ measures the slower diffusion of solute molecules whose Stokes diameters are approaching the diameter of the column-packing pores. Values of b' and ρ in the present study were obtained by best-fit matching of experimental and calculated bandwidths, based on an optimum set of values for b' and ρ. See the similar approach of ref. 13.

TABLE II

ISOCRATIC RETENTION DATA FOR ION-EXCHANGE CHROMATOGRAPHY OF LYSOZYME AND RIBONUCLEASE

Column, WCX-300 as described in Experimental. Mobile phase, blends of (a) 0.02 *M* Bis-Tris acetate and (b) 1.0 *M* sodium acetate, final pH = 6.4 (total acetate concentration *c* shown); flow-rate 1 ml/min; temperature, ambient.

Acetate concentration c (M)	*k'*	
	Ribonuclease	*Lysozyme*
0.13	11.1	
0.14	7.6	
0.15	5.0	
0.16	3.8	
0.17	3.0	
0.19	1.65	
0.22	0.93, 1.03	
0.24		14.6
0.26		8.4
0.28		6.4
0.30		4.5
0.31		4.3
0.32		3.4
0.34		2.3
0.36		2.1
0.38		1.65
0.40		1.35
0.42		1.09
0.44		0.91
0.47		0.83
0.52		0.49

Columns

Column packings were based on a 30-nm pore, 7.5 μm particle size of zirconium oxide-stabilized Zorbax® silica (Du Pont Biomedical Products, Wilmington, DE, U.S.A.), completely bonded with a monolayer of diol phase; a similar product is sold as the Zorbax Bio-Series GF-450 column for gel filtration. This column packing was further modified by introducing various functional groups into the stationary phase for ion-exchange separation. All columns were prepared by slurry packing into 8 × 0.62 cm I.D. chromatographic tubes. The columns used in this study are the Du Pont Zorbax Bio-Series SCX-300 (strong cation exchanger), WCX-300 (weak cation exchanger), and SAX-300 (strong anion exchanger), and WAX-300 (weak anion exchanger).

A pre-column between the pump and injector was used in all experiments. The pre-column consisted of a 2.0 × 0.20 cm I.D. tube (Upchurch Scientific, Oak Harbor, WA, U.S.A.) filled with 20 μm Zorbax C-8 packing (Du Pont).

TABLE III

GRADIENT RETENTION DATA FOR ION-EXCHANGE GRADIENT ELUTION OF RIBONUCLEASE AND LYSOZYME

Conditions as in Table II, t_0 = 1.88, t_D = 1.4; gradient from 0.02 *M* acetate to 1.02 *M* acetate.

Gradient time t_G *(min)*	t_g *(min)*	
	Ribonuclease	*Lysozyme*
10	5.97	8.00
20	7.68	11.42
40	10.83	17.48

RESULTS AND DISCUSSION

Experimental validation of present model for ion-exchange retention data

Both isocratic and gradient separations of lysozyme and ribonuclease were carried out, using the columns described in the Experimental section. Tables II and III summarize the resulting retention data for the weak cation exchange column (WCX-300). When the isocratic data were plotted (Fig. 1, open squares) as log k' *vs.*

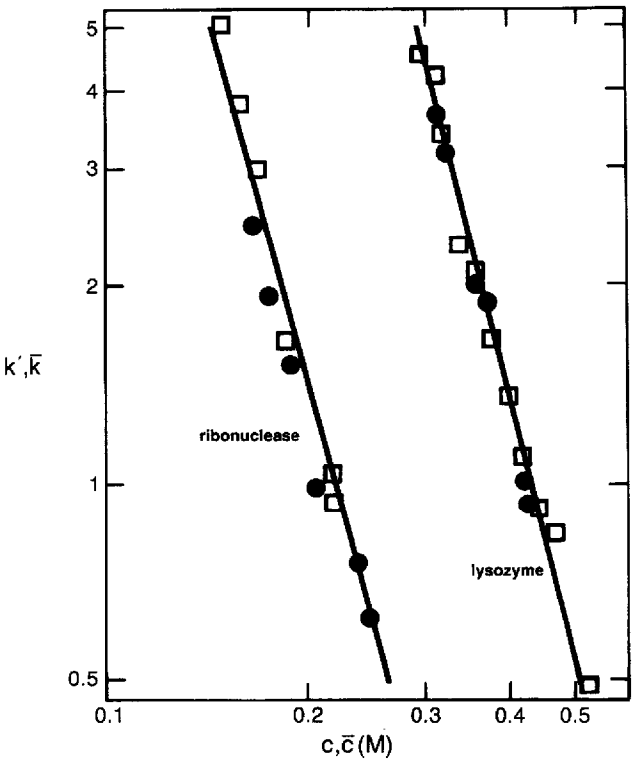

Fig. 1. Correlation of retention data from isocratic (□) and gradient elution (●). Ion-exchange chromatography of indicated proteins on weak cation-exchange column WCX-300; conditions as in Tables I and II, gradient data used to calculate values of $\bar{c}$ and $\bar{k}$ as described in text.

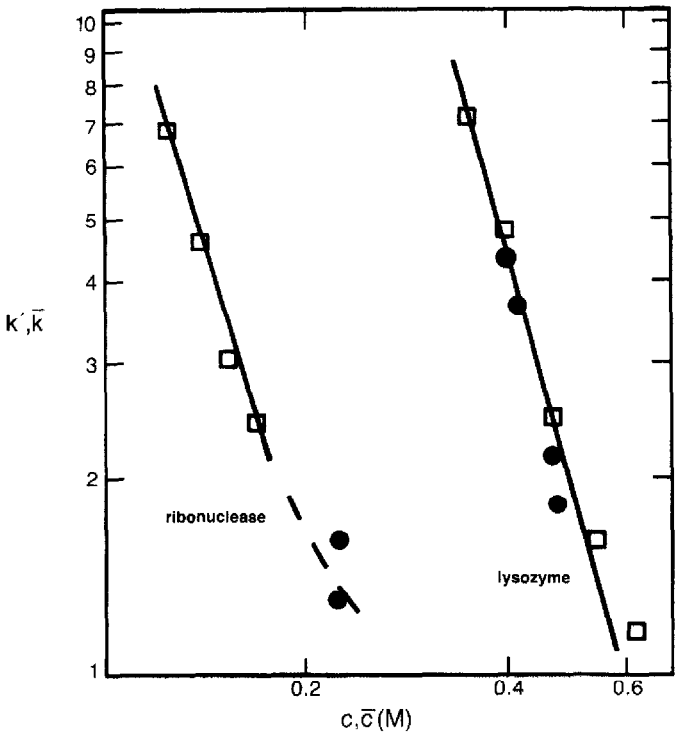

Fig. 2. Correlation of retention data from isocratic (□) and gradient elution (●). Ion-exchange chromatography of indicated proteins on strong cation-exchange column SCX-300. Conditions similar to those of Fig. 1.

log c (eqn. 4), the predicted straight-line relationship was observed. The gradient data of Table III were used to calculate values of $\bar{k}$ and $\bar{c}$, as described in the Theory section, and these values were superimposed on the plots of Fig. 1. Close agreement between isocratic and gradient data is observed, confirming the validity of the present approach. Similar agreement of this type was observed earlier for proteins separated by reversed-phase HPLC[12]. In Fig. 2, similar plots are shown for isocratic and gradient data from the strong cation-exchange column (SCX-300). Again, the agreement with eqn. 4 and between isocratic and gradient data is good.

Bandwidth data

The m-values inferred from the plots of Figs. 1 and 2 were next used with eqns. 7–10 to calculate values of σ_t for each of the gradient runs of Figs. 1 and 2. This procedure is illustrated in Appendix II. This approach requires best-fit estimates of the column parameters b' (surface diffusion) and ρ (restricted diffusion), as previously described[13] for reversed-phase separation. The resulting best-fit σ_t-values are compared with experimental values in Table IV.

The overall agreement between experimental and calculated values of σ_t in Table IV is ±12% (1 S.D.). A similar correlation[18] of bandwidth data reported by Kato *et al.*[9] for the anion-exchange separation of ovalbumin gave agreement between

TABLE IV

COMPARISON OF EXPERIMENTAL BANDWIDTH DATA WITH VALUES CALCULATED* FROM OUR MODEL FOR ION-EXCHANGE GRADIENT ELUTION

Conditions as in Tables II and III, Appendix II, or as noted.

Column	*Gradient time t_G (min)*	*Flow-rate F (ml/min)*	σ_t *(sec)*			
			Lysozyme		*Ribonuclease*	
			expt	*calc*	*expt*	*calc*
WCX-300	10	1.0	4.9	4.8	3.6	3.9
	20	1.0	6.5	6.2	4.4	4.9
	40	1.0	8.4	8.1	5.2	6.4
SCX-300	20	1.0	9.1	9.5	4.7	5.7
	40	1.0	14.1	14.1	6.8	8.1
	40	0.5	15.4	14.2	10.0	8.5
	80	0.5	22.2	20.6	12.6	12.0

* $x = 0.6$, $A = 0.6$, $b = 0.10$ (WCX-300) and 0.00 (SCX-300), $\rho = 1.0$ (WCX-300) and 0.8 (SCX-300); lysozyme, $m = 4.2$ (WCX-300), 3.8 (SCX-300); ribonuclease, $m = 3.8$ (WCX-300), 3.4 (SCX-300).

experimental and calculated σ_t values of $\pm 10\%$. The correlation of Table IV also compares favorably with the similar prediction[13] of reversed-phase bandwidths of proteins separated by gradient elution ($\pm$ 10–15%). The values of b' and ρ that result from the correlations of Table IV are physically reasonable, as will be discussed elsewhere[19]. We conclude that the correlations of Table IV and Figs. 1 and 2 provide strong support for the belief that these particular ion-exchange gradient elution separations proceed as "normal" chromatographic processes, as has been previously discussed[10]. However, we do not believe that all protein ion-exchange separations will be similarly "well behaved". It may in fact be that most such separations of larger proteins (*e.g.*, > 100 000 Daltons) exhibit anomalous behavior as shown by larger-than-predicted bandwidths. The present model allows such cases to be identified unambiguously for (a) further study and (b) attempts at improved separation (narrower bandwidths).

Use of the present model for method development

The model we have described here (further detailed in Appendix III) can facilitate method development in various ways. An example of this approach has already been presented for similar reversed-phase separations[14], where the model was used to:

(1) compare experimental σ_t values from an initial gradient experiment with values predicted by the model; abnormally large experimental σ_t values (*e.g.*, two-fold or larger) then suggest that the system is not "well behaved", which can mean that any of a number of "non-chromatographic" phenomena interfere (see discussion of ref. 20); the best approach in these cases is to minimize these non-chromatographic effects before attempting to improve the chromatographic process systematically;

(2) predict what effect a change in separation conditions will have on overall sample resolution, peak capacity, peak volume (sensitivity), etc.; this use of the model can substitute for actual experiments and maximize efficiency in method development;

(3) explore various general approaches to optimizing the separation of proteins by gradient elution ion exchange. Here, we will focus mainly on the above-mentioned options (2) and (3) for application to ion-exchange HPLC systems.

Similarities and differences in ion-exchange versus reversed-phase method development

In ref. 3 a general approach was proposed for method development in the reversed-phase gradient elution separation of peptides and proteins; this same approach can be adapted for ion-exchange gradient elution:

(1) carry out an initial separation, using a full-range gradient; *e.g.*, 0.01–0.5 *M* salt for ion exchange; the optimum gradient conditions can be inferred from the following discussion;

(2) compare average bandwidths with values predicted by the model; if experimental bandwidths are two-fold larger or more, investigate possible "chemical" as opposed to "chromatographic" remedies*;

(3) if the peaks of interest do not fall at the beginning or end of the initial chromatogram, shorten the gradient to minimize wasted time; at the same time, reduce t_G so as to maintain optimum gradient conditions as estimated initially;

(4) if the chromatogram is too crowded or overall resolution is poor, increase peak capacity by systematically increasing N while holding $\bar{k}$ constant; this can be achieved by holding b constant (eqn. 8) while increasing column length or decreasing flow-rate (*i.e.*, with increase in t_G);

(5) when peak capacity appears adequate, but some bands still overlap, change band spacing by changing $\bar{k}$ and b (change in F, other conditions held constant), or change mobile phase pH, or change the type of salt used (*e.g.* see ref. 6). We recommend this same general approach for optimizing gradient separation by ion exchange. However, a few differences from reversed-phase method development should be kept in mind.

First, it should be noted that the use of linear gradients leads to separations that are basically non-LSS. The main consequence of these non-LSS separations is that $\bar{k}$ varies with the position of a band in the chromatogram, as noted in Table I. Thus, consider the case of a gradient from 0.01–0.3 *M* salt. For solutes with the same effective charge m, assume that $\bar{k} = 5$ (a good average value in gradient elution) for a band eluted halfway through the gradient $[(t_g - t_0 - t_D)/t_G] = 0.5$. According to Table I, bands with other t_g values would have $\bar{k}$-values as shown in Table V. In general this should lead to broader elution bands at the end of the chromatogram, whereas bandwidth usually remains constant roughly from beginning to end of LSS

* We have not suggested specific ways to reduce chemical effects so as to minimize "non-well-behaved" behavior in these protein separations by gradient elution. Rather we hope that the present model will aid chromatographers in recognizing that a particular system is not well-behaved, and the same model can also assess the degree of improvement achieved by various changes in experimental conditions. Other workers (*e.g.*, Hearn *et al.*[20]) have described various "chemical" or "biochemical" effects that can lead to broader bands and poorer separation. Hopefully such systematic approaches to understanding these complex phenomena will then suggest suitable remedies.

TABLE V

VARIATION OF $\bar{k}$ WITH RETENTION TIME t_g IN ION-EXCHANGE GRADIENT ELUTION

$(t_g - t_0 - t_D)/t_G$	$\bar{k}$ (for $c_f/c_o = 30$)
0.1	19
0.3	9
0.7	3.5
1.0 (gradient end)	2.5

chromatograms*. Whenever resolution is poor near the front-end of the chromatogram, it is suggested that conditions be changed to increase $\bar{k}$ (eqns. 3 and 5) so as to determine whether $\bar{k}$ in this part of the chromatogram is too small (*i.e.*, see if resolution increases rapidly for larger $\bar{k}$).

Second, in reversed-phase (LSS) chromatography, S increases with solute molecular weight. This leads to generally narrower bands, and this tends to offset the normal increase in bandwidth for larger molecules (due to their smaller solute diffusion coefficients, D_m). As a result, bandwidth in reversed-phase HPLC tends not to increase for larger solute molecules. It is not known at the present time whether m similarly tends to increase with solute molecular weight, but there are reasons to suspect that above some minimum molecular weight (*ca.* 10 000) there is little relationship of m to M. If so, this will result in generally broader bands and poorer separation for larger molecules by ion exchange.

Finally, the predictability of values of S for solutes of known molecular weight (eqn. 22 of ref. 1) allows us to predict band broadening in reversed-phase separations without actually determining values of S for the molecules in question. Since values of m are not similarly predictable as a function of solute M-values, we must then determine m for compounds of interest if we are to predict their ion-exchange separation (bandwidths, peak capacity, resolution, etc.). This can be achieved by performing two gradient runs with different t_G-values, as described in the preceding section. Alternatively, since determination of m in this way requires rather careful work and well designed gradient equipment, many workers may prefer to simply estimate a value of m for the sample in question. Limited experience (*e.g.*, refs. 6, 9 and 21) suggests that a reasonable estimate of m for most samples is about 4.

Model calculations based on the present model

In ref. 3 we used the present model (for reversed-phase HPLC) to predict how separation changes with experimental conditions: sample molecular weight, gradient conditions (t_G, F, etc.), and a given column (the Du Pont Zorbax Bio Series PEP-RP1). In this way it was possible to develop both (a) an understanding of how peptide separations depend on experimental conditions, and (b) a general approach to sys-

* If there is a general tendency for later bands to have larger m-values, this will tend to offset this variable-$\bar{k}$ effect. Since larger m-values should in general be associated with stronger solute retention, this suggests that we may sometimes be able to ignore the practical consequences of these non-LSS gradients in ion exchange with linear gradients.

tematic method development for the gradient separation of peptides by reversed-phase HPLC.

We will follow the same approach here for the separation of proteins by ion exchange, using columns similar to those described in the Experimental section (30-nm pores, 7.5-μm particles, 8 × 0.62 cm I.D. columns). Using the present model for ion exchange separation, we will assume a standard set of gradient conditions (0.02–0.52 M salt concentration, m = 4 for the sample proteins, 25°C, etc.; see caption to Fig. 3). However, our results should be applicable to other cases as well.

We have calculated values of peak capacity PC, where

$$PC = t_G/4\,\sigma_t \tag{11}$$

Resolution will be proportional to $PC/\Delta\varphi$ as long as separation factors do not change with a change in separation conditions. This will be the case for our standard gradient conditions as long as $\bar{k}$ remains constant:

$$\bar{k} = 0.87\,t_G F/V_m\,[\log(c_f/c_0)]\,m \tag{12}$$
$$\approx V_G/V_m\,[\log(c_f/c_0)]\,m \tag{12a}$$
$$\approx [t_G/\log(c_f/c_0)]\;(F/V_m)\quad(1/m) \tag{12b}$$
$$\text{(i)}\qquad\text{(ii)}\qquad\text{(iii)}$$

As in ref. 14 we will find it convenient to first increase sample resolution by increasing $PC/\Delta\varphi$ while holding gradient volume $V_G = (t_G F)$ constant for the same column and gradient (same values of c_0 and c_f). Note also (eqn. 12b) that this equation for $\bar{k}$ can be expressed as factors (i–iii) that can be varied together while holding $\bar{k}$ constant. We will return to eqn. 12b shortly.

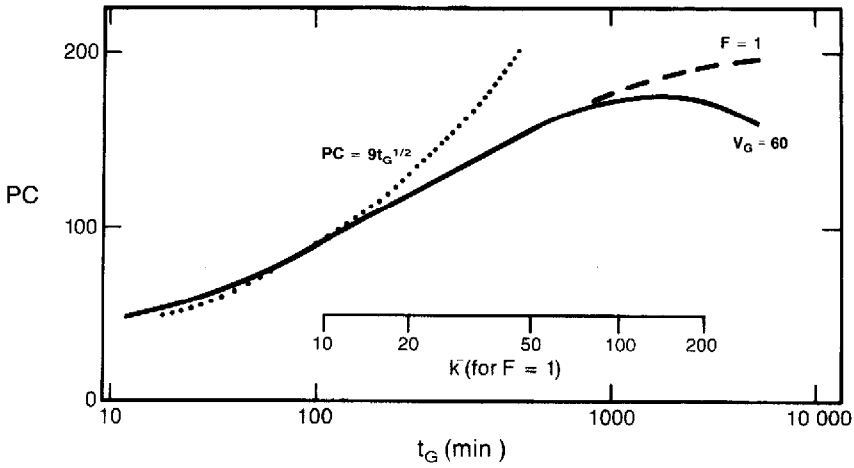

Fig. 3. Peak capacity PC (proportional to R_s) for representative ion-exchange experiments as a function of gradient time t_G, calculated for the present model. Conditions: column, 8 × 0.62 cm I.D., 30-nm pore, 7.5-μm particles; mobile phase, gradient from 0.02–0.52 M salt ($0.02 < c < 0.52$); temperature, 25°C; solute properties, m = 4, M = 10 000 D; other parameters, r = 1, x = 0.6, A = 0.6, mobile phase viscosity 1.2 cP. (——) $\bar{k}$ held constant (V_G = 60, F varying with t_G); (– – –) F held constant at 1 ml/min, t_G and $\bar{k}$ vary accordingly; (· · · · · ·) curve for PC proportional to $t_G^{1/2}$ (eqn. 13).

Effect of change in gradient time or flow-rate

Fig. 3 summarizes calculations from our model for the case of varying t_G and/or F. Two cases have been calculated: (a) increasing t_G while holding V_G constant; (b) increasing t_G while holding F constant (F = 1 ml/min). Earlier we presented[10] a simplified form of our model for reversed-phase gradient elution of proteins, and it was seen that over a range of conditions such that $1 < \bar{k} < 10$, peak capacity was given as

$$PC \propto D_m^{1/2}\, d_p^{-1}\, t_G^{1/2}\, F^0\, L^0 \tag{13}$$

That is, peak capacity and resolution increase for larger diffusion coefficients D_m (smaller molecules), smaller particles and longer separation times t_G, but flow-rate (F) or column-length (L) changes have little effect (zero-order dependence) on PC and resolution. Pretty much the same pattern is seen in the data of Fig. 3. Thus, the solid curve (V_G constant) shows F varying from 1 ml/min at t_G = 30 min to 0.01 ml/min for t = 3000 min, and the dashed curve shows F constant (1 ml/min) while t_G is changed. There is seen to be little difference in peak capacity for these two cases, showing the often (but not always) minor effect of F on PC or resolution. The square-root dependence of PC on t_G (eqn. 13) is indicated in Fig. 3 by the dotted curve, and the calculated curves follow this relationship approximately for 0.2 h < t_G < 2 h. At longer gradient times, the actual PC values increase with t_G more slowly, and for V_G constant, they approach a maximum value ($\bar{k}$ constant) at t_G = 1500 min.

The maximum value of PC ($\bar{k}$ constant) corresponds to the maximum plate number N (minimum plate height) at optimum flow-rate.

We have noted that holding V_G constant (solid curve, Fig. 3) avoids changes in band spacing and allows the systematic improvement of separation with longer gradient times (up to some maximum value of t_G, as suggested by Fig. 3). This approach also avoids increased band-broadening at higher t_G values, and contrasts in this respect with the strategy of holding F constant (dashed curve, Fig. 3). The values of $\bar{k}$ for the latter case are indicated in Fig. 3, and are seen to become quite large as t_G increases ($\bar{k} > 20$ for $t_G > 200$ min). This, in turn, results in bands having large volumes and very low peak heights. There is a price for maintaining V_G constant, however, and that is the requirement for very low flow-rates at large values of t_G (*e.g.*, F = 0.2 ml/min for a 5-h separation). With some HPLC equipment, these low flow-rates may not be practical.

Effect of change in $\bar{k}$ and column length

In Fig. 4 we have replotted the curve of Fig. 3 for V_G = 60 ml (L = 8 cm, $\bar{k}$ = 5.8). We also show a similar plot (dashed curve) for V_G = 30 ml ($\bar{k}$ = 2.9); little difference in PC as a function of t_G results for t_G < 2 h, but for larger values of t_G the peak capacity is larger for runs with larger $\bar{k}$. This is a consequence of the fundamental equation for resolution in HPLC.

$$R_s = (1/4)\,(\alpha^{-1})\, N^{1/2}\, [\bar{k}/(1 + \bar{k})] \tag{14}$$

adapted for gradient elution. For larger values of $\bar{k}/(1 + \bar{k})$, resolution and peak capacity increase proportionately.

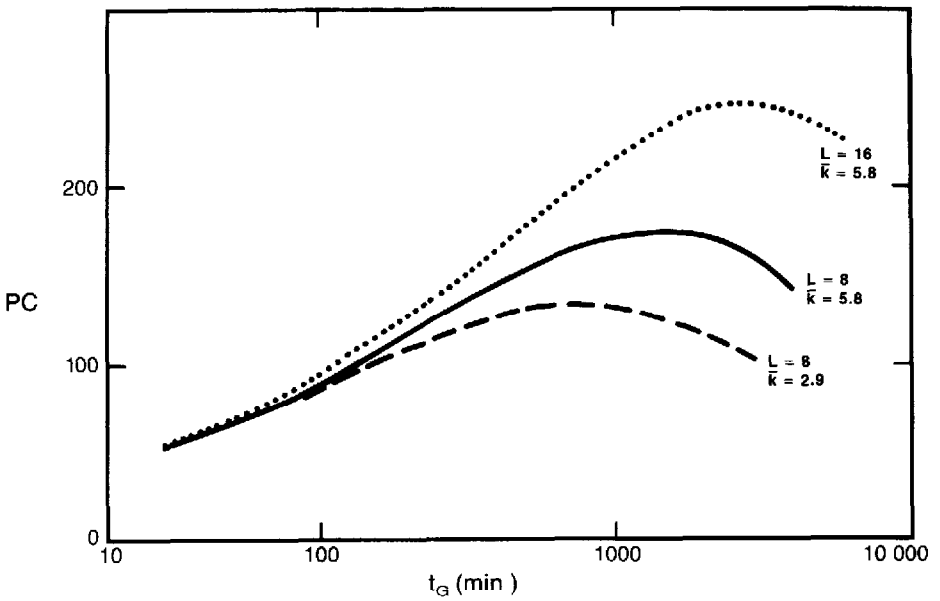

Fig. 4. Peak capacity, PC, for representative ion-exchange experiments as a function of V_G ($\bar{k}$), column length L, and gradient time t_G. Similar conditions assumed as in Fig. 3, unless otherwise noted. (——) same plot as in Fig. 3 [V_G = 60]; (– – –) similar separations, except V_G = 30 ($\bar{k}$ = 2.9); (.....) similar separations, except two columns in series (16-cm column, V_G = 120).

The dotted curve of Fig. 4 shows the effect of increasing column length while holding $\bar{k}$ and other conditions constant. In this case the solid and dotted curves should be compared, since $\bar{k}$ = 5.8 in each case, while the dotted curve is for two 8-cm column lengths in series (compared with a single column for the solid curve). As predicted by eqn. 13, column length makes little difference in peak capacity or resolution for t_G < 2 h in this example. However, for large values of t_G, values of PC and R_s on the longer column become greater than those for the shorter column. This is a consequence (eqn. 14) of the maximum value of N for the longer column being double that for the shorter column. Note, however, that maximum peak capacity with a longer column also corresponds to longer analysis times (larger t_G). The use of a two-fold increase in column length (and V_m) requires doubling the flow-rate to maintain $\bar{k}$ constant (eqn. 12), other conditions (*e.g.*, t_G) the same*.

* A reviewer has called our attention to certain other factors that arise in the case of ion-exchange protein separations. First, as opposed to reversed-phase HPLC for the *analysis* of peptide mixtures, ion exchange is usually used to isolate and purify individual proteins. Therefore purification rather than the maximization of the number of bands in the chromatogram is required. In this connection it should be noted that peak capacity and resolution are proportional to each other in gradient separations (when the gradient range, $\Delta\varphi$ is held constant)[12]. So the maximization of peak capacity (with $\bar{k}$ held constant) insures the greatest possible degree of purification.

Second, protein separations by ion exchange generally should ensure maximum recovery of bioactive material. In this case maximum resolution will not always parallel maximum recovery. Specifically, resolution is favored by long gradient times, whereas loss of bioactivity usually increases with the time spent by the sample on the column. Therefore in practical separations a compromise between these two factors must often be accepted.

Effect of sample molecular weight M

The data of Figs. 3 and 4 are for a solute with M = 10 000 D. The effect of change in the molecular weight of samples on separation in ion-exchange gradient elution is illustrated in Fig. 5. All of these runs have V_G = 60 ml ($\bar{k}$ = 5.8). Attaining a given value of PC is seen to require a larger value of t_G when the sample has a larger molecular weight. Thus, a PC of 100 is attainable for t_G = 2 h if the sample has a value of M = 10 000 D, but t_G = 8.3 h is required for a sample with M = 100 000 D. This is a direct consequence of the smaller diffusion coefficients (D_m) and resulting larger values of reduced velocity (v) for larger solute molecules; *cf.* eqn. 13.

Note also in Fig. 5 that the maximum peak capacity attainable for solutes where 10 000 < M < 100 000 is about the same. The reason is that for the ion-exchange separations of native proteins on a 30-nm pore packing, the diffusion of samples in this molecular weight range is not seriously affected by pore size. That is, a 30-nm pore packing is large enough for native proteins in this size range.

Effect of charge m on solute molecules

Fig. 6 illustrates the effect of a change in m on peak capacity, other conditions being the same. A larger value of m corresponds to lower values of $\bar{k}$, but the effect of this on peak capacity is compensated by narrower bands, and an overall increase in PC. At a given mobile phase pH, the m-values of different solutes are expected to remain constant. However, if the pH is changed, m usually increases or decreases in regular fashion: m increases with pH for anion exchange, and m decreases with pH for cation exchange. This would suggest generally higher pH values for anion exchange, and lower pH values of cation exchange, which is the usual practice (*e.g.*, pH of about 6 for cation exchange, 8 for anion exchange). However, the major effect of change in pH will usually be a change in band-spacing within the chromatogram

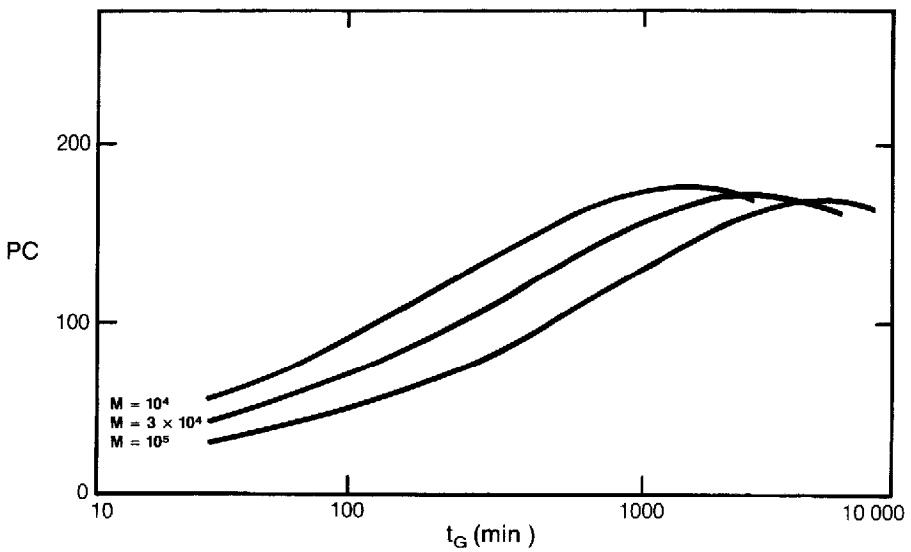

Fig. 5. Peak capacity PC for representative ion-exchange experiments as a function of the molecular weight of the sample. Similar conditions assumed as in Fig. 3, unless otherwise noted.

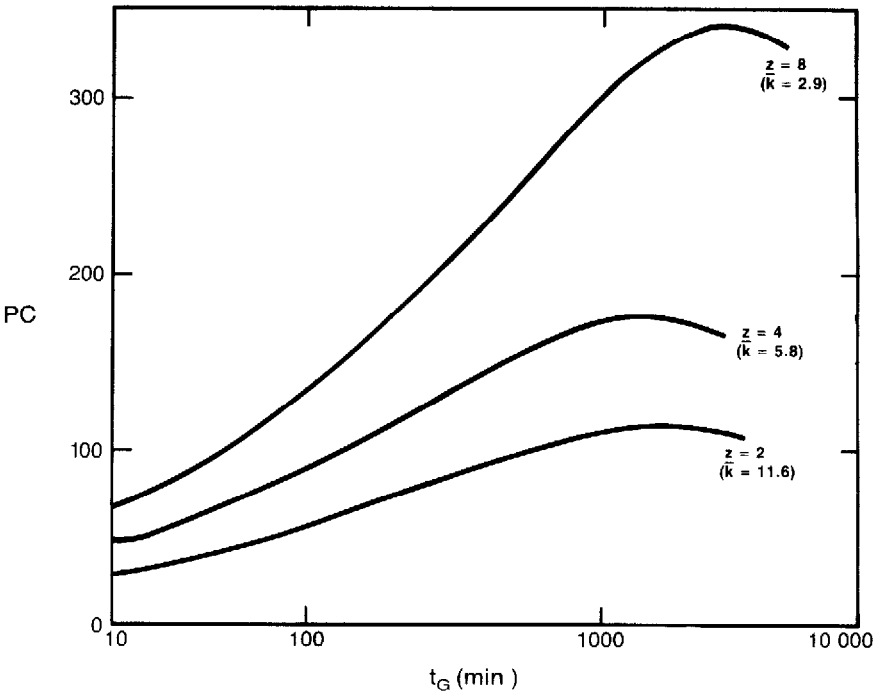

Fig. 6. Peak capacity PC for representative ion-exchange experiments as a function of protein charge m. Similar conditions assumed as in Fig. 3, unless otherwise noted.

(change in α), and this effect will often dictate what pH is optimal for a given sample and column.

The use of Figs. 3–6 for method development

Figs. 3–6 illustrate the trends in peak capacity and resolution as experimental conditions are changed for the separation of proteins by ion-exchange gradient elution. In many cases, we may not know the exact charge m on various protein molecules, nor even the molecular weight of the sample. However, it can be seen in Figs. 5 and 6 that the general change in PC with gradient time is the same, regardless of M or m. Thus, following an initial gradient run, separation conditions can always be varied as suggested by Fig. 4 to improve overall resolution, while holding $\bar{k}$ constant.

Fig. 4 suggests that an increase in gradient time t_G will be generally useful in improving overall resolution, if the flow-rate is reduced in proportion to t_G (and V_m) so as to hold $\bar{k}$ constant ($\bar{k} \approx 5$). However, Fig. 4 also indicates that maximizing peak capacity and resolution can require long separation times: 10 h or more per run. In this sense the application of modern HPLC to protein separations seems to have retrogressed to the early days of protein separations. Actually, this does not have to be the case. In general, we require adequate resolution for one or more bands in the sample, but it is less common that the same peak capacity is required for all parts of the chromatogram.

As an example, the initial gradient might be from 0.02–0.50 M salt, similar to

Fig. 4, but a 2-h chromatogram (PC $\cong$ 95) might give insufficient separation of a band that is eluted half-way through the gradient. Further increase in PC at this point in the chromatogram can be achieved by focusing attention on a shorter gradient that overlaps the peak(s) of interest.

In the simplest case, assume that the sample is to be re-chromatographed so as to isolate only the peak of interest (which is eluted at about 0.25 M salt). In this case, we can use a narrower gradient, starting at a larger value of c_0 and ending at a smaller value of c_f. Assuming an average value of $m = 4$, and assuming (a) that k_0 for the sample band should be at least $k' = 20$ for $c = c_0$, and (b) $\bar{k} = 5$, eqn. 4 suggests that c_0 should be less than 0.25 M by a factor of $(5/20)^{1/4}$*, or about 0.7-fold. That is, $c_0 = 0.25 \times 0.7 = 0.18$ M. The gradient can be terminated shortly after elution of the band, so $c_f \approx 0.27$ M. Referring to eqn. 12b, we can maintain $\bar{k}$ constant (other conditions being the same), while changing t_G in proportion to log (c_f/c_0). The old value of log (c_0/c_f) = log (0.5/0.02) = 1.40. The new value of log (c_f/c_0) = log (0.27/0.18) = 0.18, which is a reduction by a factor of 0.18/1.4 = 0.13. This means that the new run can be carried out with $t_G = 120 \times 0.13 = 16$ min, *vs.* 2 h for the original run. More important, referring to Fig. 4, we can further increase PC and relative resolution now by increasing t_G, but the narrower gradient range means that significant improvement in separation can be achieved within a reasonable run time. For example, the original PC-value of 95 (pro-rated over the new gradient range) could have been doubled with a run time of 10 h, using a 16-cm column (two 8-cm columns in series) and conditions for $\bar{k} = 5.8$ (Fig. 4). However, with the new gradient range of 0.18–0.27 M, the gradient time t_G is now only 1.3 h or 80 min**.

In the past, a similar strategy has been adopted by protein chemists, simply by running a shallower gradient in the vicinity of bands that are more difficult to resolve. The same practice is obviously usable in terms of our approach, except that we would recommend that the flow-rate be decreased in conjunction with shallower gradients, so as to maintain $\bar{k}$ constant (and optimal).

An example of the present approach to method development for protein separations by ion-exchange gradient elution

Fig. 7 illustrates the present approach as applied to a mixture of crude ovalbumin. In the first chromatogram a wide-range gradient is used (0.02–1.02 M acetate) with an experimental anion-exchange column (SAX-300), similar to the column assumed in Fig. 5. It is known that $M = 44\,000$ for this sample, and m was estimated equal to 4 (the actual value is about 6, but this would often not be known for a particular sample). Initial conditions were selected to give $\bar{k} \approx 5$: $t_G = 50$ min, $F = 1$ ml/min (eqn. 12a, $\bar{k} = (50 \times 1)/1.6 \times [\log (1.02/0.02)] \times 4 = 4.6$. The resulting initial separation is shown in Fig. 7a, and it is seen that the sample is poorly resolved. It is also seen that the main peaks fall within a narrow range in the middle of the gradient.

---

* From eqn. 4 we have log c = (log K)/m − (1/m) log k'. For k'-values $\bar{k}$ and k_0 corresponding to c-values "c-band" and c_0, the latter relationship yields: c_0 = c-band × $(\bar{k}_0)^{1/m}$; which for the present example becomes: $c_0 = 0.25 \times (5/20)^{1/4} = 0.18$.

** In this discussion we are really interested in resolution R_s, but since the pro-rated (full-gradient) value of PC is proportional to R_s, we can increase R_s by increasing PC.

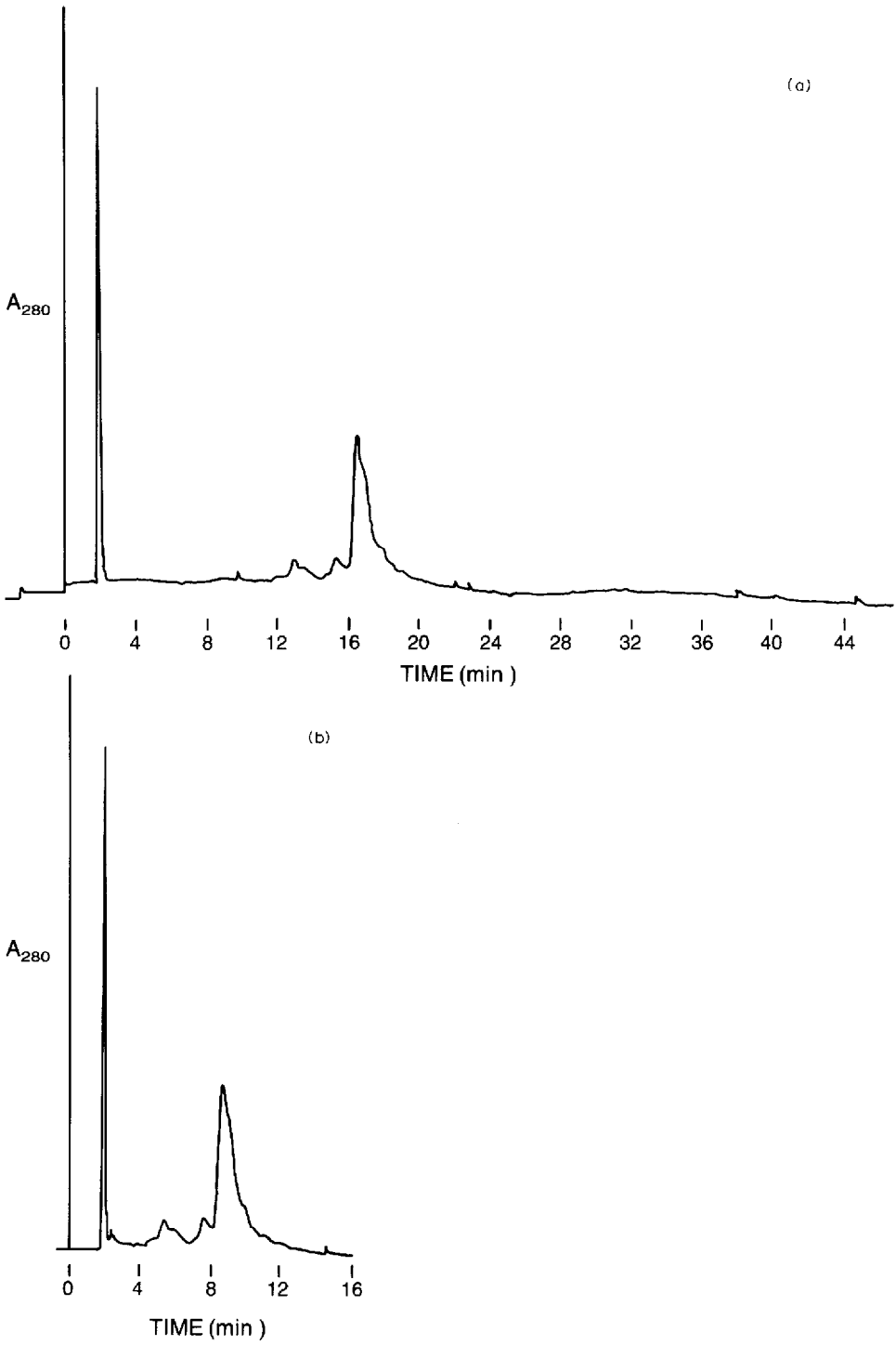
(a)
A_{280}
0
4
8
12
16
20
24
28
32
36
40
44
TIME (min)
(b)
A_{280}
0
4
8
12
16
TIME (min)

Fig. 7.

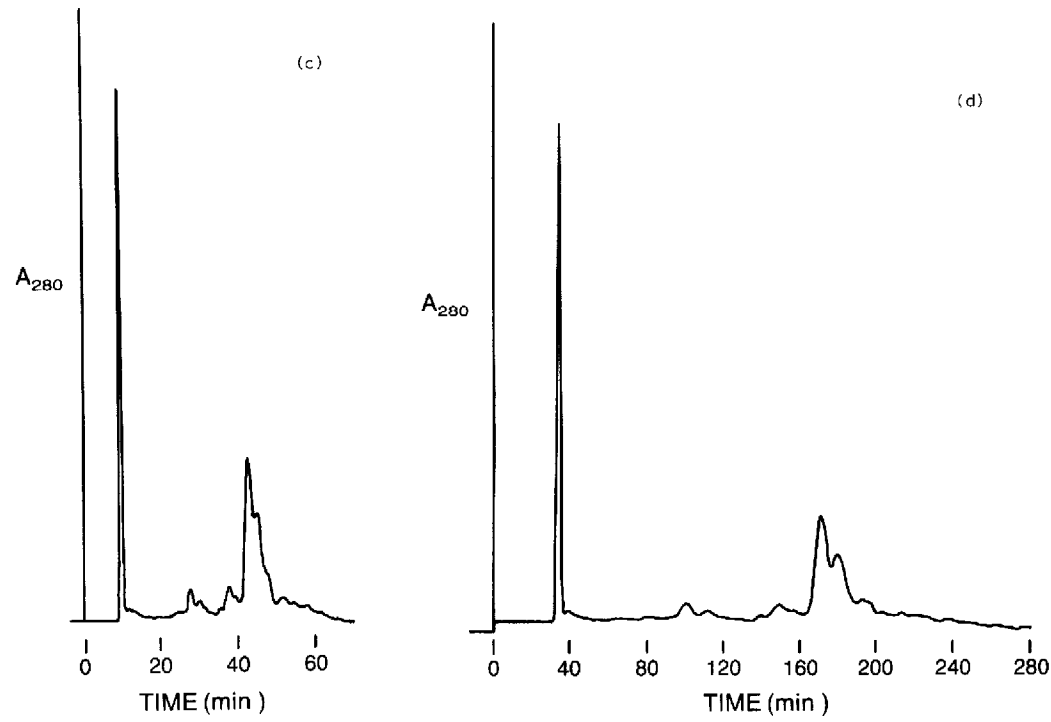

Fig. 7. Experimental example of present approach to optimizing the ion-exchange gradient elution separation of proteins. Separation of crude ovalbumin on SAX-300 column. Conditions: sample size, 25 μg in 25 μl; ambient temperature; gradient solvents as in Table III; one 8.0 × 0.62 cm I.D. column unless otherwise noted. (a) 0.02–1.02 *M* salt gradient in 50 min, F = 1 ml/min; (b) 0.10–0.30 *M* gradient in 14 min, F = 1 ml/min; (c) 0.10–0.30 *M* gradient in 70 min, F = 0.2 ml/min; (d) 0.10–0.30 *M* gradient in 280 min, F = 0.1 ml/min, two columns (L = 16 cm) in series.

In the next separation, the gradient range was narrowed, while holding $\bar{k}$ constant. From the retention times of bands in Fig. 7a, a new gradient range of 0.17–0.47 *M* acetate was selected. The gradient time was also shortened to maintain $\bar{k}$ constant (eqn. 12b), holding other conditions constant. This means that t_G must be reduced in proportion to log (c_f/c_0): by 0.46/1.70 = 0.26-fold = 50 min × 0.26 = 13 min. The result (t_G = 14 min) in Fig. 7b shows the sample filling most of the chromatogram during the gradient.

Now resolution can be increased by increasing gradient time five-fold, to t_G = 70 min. The flow-rate must be simultaneously decreased five-fold, to 0.2 ml/min. The result is shown in Fig. 7c, and the increase in sample resolution is apparent. At this point we require further improvement in peak capacity, and from Fig. 4 it appears that an increase in gradient time t_G and column length L is now appropriate (on a gradient-range corrected basis, t_G for the run of Fig. 7c is about 200 min). Our next run (Fig. 7d) provides a further increase in t_G to 280 min, with an increase in column length to 16 cm (two columns in series). The flow-rate (0.2 ml/min) must be decreased four-fold for the increase in t_G, but increased two-fold for the doubling of

column length and V_m: thus $F = 0.10$ ml/min. At this point in the separation (Fig. 7d), a reasonable resolution of the two major bands (and most of the minor bands) has resulted. If desired, further improvement in the separation could be achieved by further increase in peak capacity, and/or by change in band spacing by changing either $\bar{k}$ (via change in F) or pH.

Although the present approach results in considerable improvement in the separation of this ovalbumin sample, it appears that this separation is not "well behaved". Thus, the observed value of σ_t for the major peak in Fig. 7d is about 4 min, whereas the present model predicts a value of about 1.1 min. A failure of these separations (Fig. 7) to follow the present model quantitatively is also indicated by a slower-than-predicted increase in resolution from the run of Fig. 7b to that of Fig. 7d: R_s actually increases by a factor of about 1.4, compared to a factor of 3 predicted by the model. This is typical of systems that are not "well behaved", where chromatography is subject to various interfering physicochemical processes. Interestingly, the separation of ovalbumin in the system of Kato *et al.*[9] (see also ref. 18) does not appear to exhibit any such anomaly.

Note for the sample of Fig. 7 that the initial resolution did not allow an estimate of σ_t to compare with the model. Thus the non-ideal behavior in this system could only be recognized after some further attempts at improving resolution. However, we can estimate that the value of σ_t for ovalbumin in the run of Fig. 7a is about 1.7 times greater than the model predicts.

Bandwidths in isocratic ion-exchange HPLC

Limited isocratic bandwith data were collected for lysozyme separated under similar conditions on the WCX-300 column. These data are summarized in Table VI. Using the column parameters from the fitting of our model to the present gradient data for lysozyme (Table IV), it was possible to calculate values corresponding to the conditions of Table VI. These calculated values of N are only roughly in agreement with experimental values, as seen from the ratios of experimental and calculated σ_t values: $(\sigma_{expt}/\sigma_{calc}) = 1.25 \pm 0.09$. Experimental values of N tend to be significantly

TABLE VI

COMPARISON OF EXPERIMENTAL PLATE NUMBERS FOR ISOCRATIC ELUTION OF LYSOZYME FROM WCX-300 COLUMN WITH VALUES FROM PRESENT MODEL

Conditions and column parameters (A, b', ρ) similar to values of Table II, flow-rate = 1.0 ml/min.

c (M)	k'	N		$(\sigma_{expt}/\sigma_{calc})$
		expt	*calc**	
0.455	0.87	920	1530	1.29
0.41	1.22	1210	1464	1.10
0.37	1.86	890	1440	1.27
0.33	2.85	830	1479	1.34
0.305	4.40	1200	1600	1.15
0.27	7.4	1030	1850	1.34

* Similar calculation as in Appendix II.

higher than calculated values in this case, and limited data of ours for other ion-exchange columns suggest that this is generally true (isocratic runs are less efficient than corresponding gradient runs). We will comment further on this elsewhere[19].

CONCLUSIONS

The LSS model previously developed for the reversed-phase gradient elution separation of proteins has now been extended to ion-exchange protein separations with linear gradients. These separations are non-LSS in nature, but this has little practical effect on the understanding and control of sample resolution and method development. An exact treatment is described for using two or more gradient runs to predict isocratic elution in corresponding ion-exchange systems as a function of experimental conditions. Comparison of predicted isocratic retention for lysozyme and ribonuclease (from gradient runs) with directly measured isocratic retention shows good agreement.

The use of gradient runs also allows the measurement of the effective charge m on the protein molecule in an ion exchange system. With a value of m thus obtained, the model allows the prediction of bandwidths in ion-exchange gradient elution. Comparison of experimental bandwidths with values thus calculated from the model shows good agreement ($\pm 12\%$, 1 S.D.). Further comparison of isocratic bandwidths with values predicted from the model shows somewhat poorer agreement ($\pm 25\%$, 1 S.D.). It should be emphasized, however, that similar agreement is not expected in every ion-exchange protein separation. Many such systems are known to be "non-well-behaved" (*e.g.* ref. 21), and cases of this type will be apparent when bandwidths are compared with values predicted by the present model. A two-fold or greater discrepancy in such comparisons (experimental bandwidths wider than predicted) indicates that chemical effects dominate; the appropriate strategy then is to modify the chemistry of the system before proceeding with chromatographic optimization.

With the present model thus validated, it is possible to use the model to predict how ion-exchange separation varies with experimental conditions and the nature of the sample (charge m and molecular weight M). Preliminary calculations of this type confirm previous experience in showing that for short run times (< 2 h), mobile phase flow-rate F and column length L have little effect on peak capacity or average resolution. However, for longer run times, the model shows that both F and L can affect resolution significantly.

On the basis of our findings, a general approach to developing an ion-exchange protein separation is outlined. The resolution of crude ovalbumin on an anion-exchange column is used to illustrate this method development scheme.

APPENDIX I

Use of two gradient runs to determine isocratic retention parameters

We will use the lysozyme retention data of Table III to illustrate this approach. For two initial gradient runs, with $t_G = 10$ and 20 min, respectively, we have retention times for lysozyme in each run: t_G (10 min): $t_{g1} = 8.00$ min; t_G (20 min): $t_{g2} = 11.42$ min. Other system parameters are: $t_0 = 1.88$ min, $t_D = 1.40$ min, $t_{G2}/t_{G1} = \beta = 2$.

TABLE A1

EXAMPLE OF CALCULATION OF σ_t

Parameter	*Reference*	*Value*
Column dead volume V_m	ref. 1, eqn. 12	1.61 ml
Mobile phase velocity u	ref. 1, eqn. 26	0.0828 cm/s
Solute D_m value	ref. 1, eqn. 23–25	$9.94 \cdot 10^{-7}$ cm/s
Reduced velocity v	ref. 1, eqn. 18	62.5
b_0	*	
$\bar{k}$	eqn. 5	1.32
Knox parameter B	ref. 1, eqn. 21	1.23
Knox parameter C	ref. 1, eqn. 19, 20	0.0790
Reduced plate height h	ref. 1, eqn. 16	7.33
Column plate number N	ref. 1, eqn. 15, 17	1454
J-factor	ref. 2, eqn. 12	1.65
G-factor	ref. 14, eqn. 25a, c	0.691
σ_t	eqn. 7	4.79 s

* Calculation of b_0. This is an iterative procedure which is described in ref. 18. A value of b is calculated first, using eqn. 8: $b = 1.156$ for the present case. Now, a value of $\bar{c}$ is estimated, using the latter value of b and eqn. 8. The resulting value of $\bar{c}$ is then used with eqn. 10 to estimate r, and from r an improved value of b_0 is determined from eqn. 9. The procedure is repeated until consecutive values of b_0 are sufficiently close. For the present case, we have the following calculated results: Step 1, $\bar{c} = 0.477$, $r = 0.533$, $b_0 = 0.616$; Step 2, $\bar{c} = 0.440$, $r = 0.578$, $b_0 = 0.668$; Step 3, $\bar{c} = 0.446$, $r = 0.570$, $b_0 = 0.659$. The third iteration, $b_0 = 0.659$, is acceptable.

We now calculate b for the 10-min run (b_1) as (eqn. 13 of ref. 17)

$$b_1 = (t_0 \log \beta)/[t_{g1} - (t_{g2}/\beta) - (t_0 + t_D)(\beta - 1)/\beta] \quad \text{(A1)}$$

This yields $b_1 = 0.871$, and a similar treatment for b_2 gives $b_2 = 0.435$ (b_2 will always equal b_1/β).

We next determine $\bar{k}$ for each gradient run from eqn. 5: $\bar{k}_1 = 1.00$, $\bar{k}_2 = 2.00$. The corresponding values of $\bar{c}$ are given by eqn. 6: $\bar{c}_1 = 0.427\ M$, $\bar{c}_2 = 0.362\ M$. These values of $\bar{k}$ *vs.* $\bar{c}$ are plotted in Fig. 1 (●) for the lysozyme curve.

A value of m can now be determined from two sets of ($\bar{c}$, $\bar{k}$) values by solving eqn. 4 for m and k: $m = \log(\bar{k}_2/\bar{k}_1)/\log(\bar{c}_1/\bar{c}_2) = 4.20$. However, the resulting value of m from only two gradient runs will be in error by $+0.3$ units. Therefore, a corrected value of m should be determined by subtracting 0.3 units from the gradient-derived value of m[17], yielding $m = 3.90$ (experimental value, 4.2).

APPENDIX II

Calculation of exact values of bandwidth in ion-exchange gradient elution, given a value of m

The model we have used is described in refs. 12, 13 and 18 and the present paper. We will outline the approach here for calculating exact values of σ_t, using an example from Table IV (WCX-300 column, gradient time of 10 min).

The experimental input parameters are as follows: column length L, 8 cm;

column diameter d_c, 0.62 cm; column porosity x, 0.60; particle diameter d_p, 0.00075 cm; separation temperature T, 25°C; mobile phase viscosity at 25°C (water), 0.89 cP; sample molecular weight, 13 000; initial salt concentration c_0, 0.02 M; final salt concentration c_f, 1.02 M; solute–salt charge ratio m, 4.2 (determined from Fig. 2); mobile phase flow-rate F, 1.0 ml/min = 0.0167 ml/s; gradient t_G, 10 min; solute retention time t_G, 8.00 min.

Additionally, the various column parameters (A, b' and ρ) must be known. In the present study for the systems of Table IV, a value of $A = 0.6$ (a well-packed column) was assumed, and values of b' were the best fit to the experimental data of Table IV for each column (WCX-300 and SCX-300). For the present column (WCX-300), $b' = 0.10$ and $\rho = 1.00$. The steps in calculating σ_t are now as shown in Table A1.

APPENDIX III

Calculation of data for Figs. 3–6

Peak capacity values *vs.* experimental conditions were calculated from eqn. 11, using values of σ_t determined as in Appendix II. The only change is that values of b' and ρ were estimated from protein molecular weight M for 30-nm pore columns of the type under discussion (see Experimental section). The relationship of b' and ρ to M is described in ref. 18. For the present columns this relationship becomes

$$b' = 0.17 - 0.03 \log M \quad \text{(A2)}$$

$$\rho = 1.45 - 0.18 \log M \quad \text{(A3)}$$

A model calculation is described below, based on the same format as Appendix II.

Inputs to the calculation are as follows: $L = 8$ cm; $d_c = 0.62$ cm; $d_p = 0.00075$ cm; $T = 25$°C; viscosity = 0.89 cP; $M = 10\,000$; $c_0 = 0.02$ M; $c_f = 0.52$ M; $m =$

TABLE A2

EXAMPLE OF CALCULATION OF PC (FIGS. 3–6)

Parameter	*Reference*	*Value*
V_m	Same	1.61
u	Same	0.166
D_m	Same	$1.09 \cdot 10^{-6}$
v	Same	113.4
b_0	*	0.152
k	Same	5.72
B	Same	1.374
C	Same	0.1279
h	Same	17.42
N	Same	612
J	Same	1.219
G	Same	0.897
σ_t	Same	8.24
PC	eqn. 11	54.6

* Calculation of b_0. The value of b (eqn. 8) is 0.152, and since r is taken equal to 1, the value of $b_0 = 0.152$. This corresponds to an average value of $b_0 = 0.152$ for the entire chromatogram.

4; F = 2 ml/min; t_G = 30 min; an average solute retention time was assumed, such that r = 1. For the column parameters, A was assumed equal 0.6, and b' (0.048) and ρ (0.713) were calculated from eqns. A2 and A3 (see Table A2).

SYMBOLS

b	gradient steepness parameter (eqns. 1, 3 and 8)
b_0	value of b at a particular time during ion-exchange gradient elution (eqns. 9 and 10)
b'	surface diffusion parameter (ref. 12)
c	concentration (molarity) of salt in the mobile phase (ion-exchange separation)
$\bar{c}$	average or effective value of c for gradient elution; $\bar{c}$ and $\bar{k}$ correspond to values for the sample band when it reaches the column midpoint
c_f	final value of c in an ion-exchange gradient
c_0	initial value of c in an ion-exchange gradient
D_m	solute diffusion coefficient in the mobile phase (cm^2/s)
d_p	particle diameter of column-packing (cm)
F	mobile phase flow-rate (ml/s or ml/min)
G	gradient compression factor (ref. 11)
J	anomalous band-broadening factor for gradient elution; experimental values of σ_t are larger than experimental values by the factor J (ref. 13)
K	ion exchange distribution constant (eqn. 4)
k'	capacity factor
$\bar{k}$	effective or average value of k' in gradient elution (eqn. 5)
k_i	k' at the column inlet during gradient elution (eqn. 1)
k_0	value of k' at the beginning of gradient elution (eqn. 1)
L	column length (cm)
LSS	linear-solvent-strength gradient elution (eqn. 1)
m	effective charge on solute molecule (eqn. 4)
N	column plate number
PC	peak capacity; number of separated bands (R_s = 1) that will fit into a chromatogram (for gradient elution, the chromatogram is defined by time t_G)
r	ratio of actual b-value to average b-value (b_0) (eqns. 9 and 10)
R_s	resolution function, equal to the difference in retention times for two adjacent bands, divided by their average bandwidths
S	change in k' with the mobile phase composition φ in isocratic reversed-phase separation; $S = \mathrm{d}(\log k')/\mathrm{d}\varphi$
t	time after sample injection and start of gradient (s or min)
t_D	dwell time of gradient elution system (see ref. 15) (s or min)
t_g	retention time in gradient elution (s or min)
t_G	gradient time (s or min)
t_0	column dead-time (s or min)
V_G	gradient volume, equal to $t_G F$ (ml)

V_m	column dead-volume (ml)
α	separation factor (ratio of k'-values for adjacent bands)
φ	volume-fraction of organic solvent in a reversed-phase eluent
Δc	change in c during ion-exchange gradient; equal to $(c_f - c_0)$
$\Delta\varphi$	change in φ from beginning to end of a reversed-phase gradient
ρ	restricted-diffusion parameter (ref. 12)
σ_t	bandwidth (1 S.D.) in gradient elution (s)
σ_{expt}, σ_{calc}	experimental or calculated value of σ_t

REFERENCES

1 A. J. Alpert and F. E. Regnier, *J. Chromatogr.*, 185 (1979) 375.
2 F. E. Regnier and K. M. Gooding, *Anal. Biochem.*, 103 (1980) 1.
3 L. Soderberg, J. Bergstrom, K. Anderson, A. Bergwall, H. Lindblom and K. A. Hansson, in H. Peeters (Editor), *Protides of the Biological Fluids, Proc. 30th Coll., Brussels, 1982*, Vol. 30, Pergamon Press, Oxford, 1983, p. 629.
4 Y. Kato, K. Nakamura and T. Hashimoto, *J. Chromatogr.*, 266 (1983) 385.
5 P. Lundal, E. Greijer, H. Lindblom and L. G. Fägerstam, *J. Chromatogr.*, 297 (1984) 129.
6 W. Kopaciewicz, M. A. Rounds, J. Fausnaugh and F. E. Regnier, *J. Chromatogr.*, 266 (1983) 3.
7 F. C. Nachod (Editor), *Ion Exchange. Theory and Application*, Academic Press, New York, 1949.
8 K. M. Gooding and M. N. Schmuck, *J. Chromatogr.*, 296 (1984) 321.
9 Y. Kato, K. Komiya and T. Hashimoto, *J. Chromatogr.*, 246 (1982) 13.
10 L. R. Snyder, M. A. Stadalius and M. A. Quarry, *Anal. Chem.*, 55 (1983) 1412A.
11 L. R. Snyder, in Cs. Horváth (Editor), *High-Performance Liquid Chromatography*, Vol. 1, Academic Press, New York, 1980, p. 208.
12 M. A. Stadalius, H. S. Gold and L. R. Snyder, *J. Chromatogr.*, 296 (1984) 31.
13 M. A. Stadalius, H. S. Gold and L. R. Snyder, *J. Chromatogr.*, 327 (1985) 27.
14 M. A. Stadalius, M. A. Quarry and L. R. Snyder, *J. Chromatogr.*, 327 (1985) 93.
15 M. A. Quarry, R. L. Grob and L. R. Snyder, *J. Chromatogr.*, 285 (1984) 1.
16 M. A. Quarry, R. L. Grob and L. R. Snyder, *J. Chromatogr.*, 285 (1984) 19.
17 M. A. Quarry, R. L. Grob and L. R. Snyder, *Anal. Chem.*, submitted for publication.
18 M. A. Stadalius, B. F. D. Ghrist, D. Kritcherki and L. R. Snyder, *J. Chromatogr.*, to be submitted.
19 M. A. Stadalius, B. F. D. Ghrist and L. R. Snyder, *J. Chromatogr.*, to be submitted.
20 M. T. W. Hearn, A. N. Hodder and M.-I. Aguilar, *J. Chromatogr.*, 327 (1985) 47.
21 R. W. Stout, S. I. Sivakoff, R. D. Ricker, H. C. Palmer, M. A. Jackson and T. J. Odiorne, *J. Chromatogr.*, 352 (1986) 381.